characterizing yielding as well as hardening of the material. The yield criterion is therefore expressed as

$$J_2^3 - 2.25 J_3^2 = k^6 \tag{2.164}$$

where k is the yield stress in pure shear, which is related to the yield stress σ_0 in simple tension by

$$k = \sqrt[6]{\tfrac{2}{81}}\,\sigma_0 = 0.54\sigma_0 \tag{2.165}$$

Comparing to $k = 0.5\sigma_0$ of Tresca and $k = 0.577\sigma_0$ of von Mises, the yield stress in pure shear falls between the values predicted by Tresca and von Mises. The yield curve of Eq. (2.165) as plotted in Fig. 2.13 does lie between the Tresca hexagon and the von Mises circle and passes through most of the experimental points.

2.3. Failure Criterion for Pressure-Dependent Materials

2.3.1. Characteristics of the Failure Surface of an Isotropic Material

Failure of a material is usually defined in terms of its load-carrying capacity. However, for perfectly plastic materials, yielding itself implies failure, so the yield stress is also the limit of strength.

As in the case of the yield criteria, a general form of the failure criteria can be given by Eq. (2.130) for anisotropic materials and by Eqs. (2.131) through (2.133) for isotropic ones. As we already know, yielding of most ductile metals is hydrostatic pressure independent. However, the behavior of many nonmetallic materials, such as soils, rocks, and concrete, is characterized by its hydrostatic pressure dependence. Therefore, the stress invariant I_1 or ξ should not be omitted from Eq. (2.132) and Eq. (2.133), respectively.

The general shape of a failure surface, $f(I_1, J_2, J_3) = 0$ or $f(\xi, \rho, \theta) = 0$, in a three-dimensional stress space can be described by its cross-sectional shapes in the deviatoric planes and its meridians in the meridian planes. The cross sections of the failure surface are the intersection curves between this surface and a deviatoric plane which is perpendicular to the hydrostatic axis with $\xi = \text{const}$. The meridians of the failure surface are the intersection curves between this surface and a plane (the meridian plane) containing the hydrostatic axis with $\theta = \text{const}$.

For an isotropic material, the labels 1, 2, 3 attached to the coordinate axes are arbitrary; it follows that the cross-sectional shape of the failure surface must have a threefold symmetry of the type shown in Fig. 2.19b. Therefore, when performing experiments, it is necessary to explore only the sector $\theta = 0°$ to $60°$, the other sectors being known by symmetry.

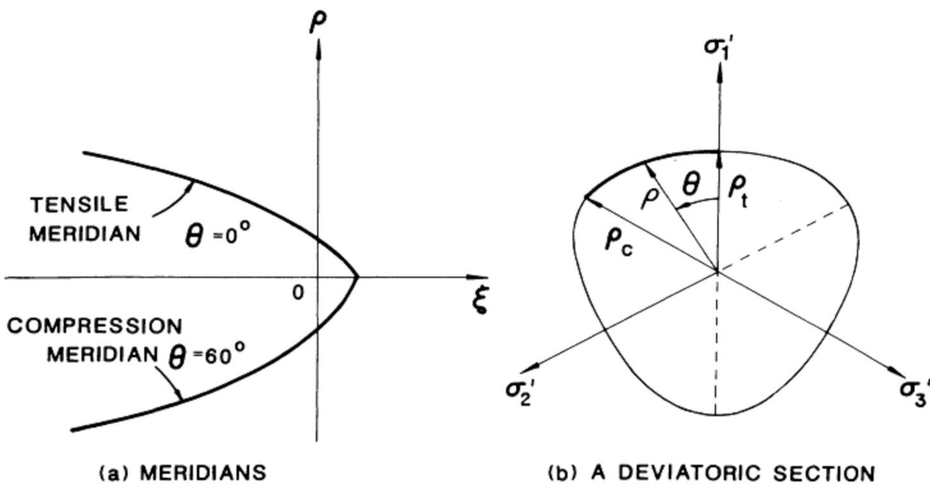

FIGURE 2.19. General shape of the failure surface for an isotropic material.

The typical sector shown in Fig. 2.19b by a heavy line corresponds to the regular ordering of the principal stresses, $\sigma_1 \geq \sigma_2 \geq \sigma_3$. Within this ordering, there are two extreme cases:

$$\sigma_1 = \sigma_2 > \sigma_3 \tag{2.166}$$

and

$$\sigma_1 > \sigma_2 = \sigma_3 \tag{2.167}$$

corresponding to $\theta_1 = 60°$ and $\theta_2 = 0°$, respectively. To show this, we substitute Eqs. (2.166) and (2.167) into Eq. (2.115) and get

$$\cos\theta_1 = \frac{\sqrt{3}}{2}\frac{s_1}{\sqrt{J_2}} = \frac{2\sigma_1 - \sigma_1 - \sigma_3}{2\sqrt{3}\sqrt{\frac{2}{6}(\sigma_1 - \sigma_3)^2}} = \frac{1}{2}$$

and

$$\cos\theta_2 = \frac{2\sigma_1 - \sigma_3 - \sigma_3}{2\sqrt{3}\sqrt{\frac{2}{6}(\sigma_1 - \sigma_3)^2}} = 1$$

respectively. The meridian corresponding to $\theta_1 = 60°$ is called the *compression meridian* in that Eq. (2.166) represents a stress state corresponding to a hydrostatic stress state with a compressive stress superimposed in one direction. The meridian determined by $\theta = 0°$, corresponding to Eq. (2.167), represents a hydrostatic stress state with a tensile stress superimposed in one direction and is therefore called the *tensile meridian.*

Furthermore, the meridian determined by $\theta = 30°$ is sometimes called the *shear meridian.* It also follows from the definition of $\cos\theta$ in Eq. (2.115) that this equation is fulfilled for $\theta = 30°$, when the stresses are σ_1, $(\sigma_1 + \sigma_3)/2$,

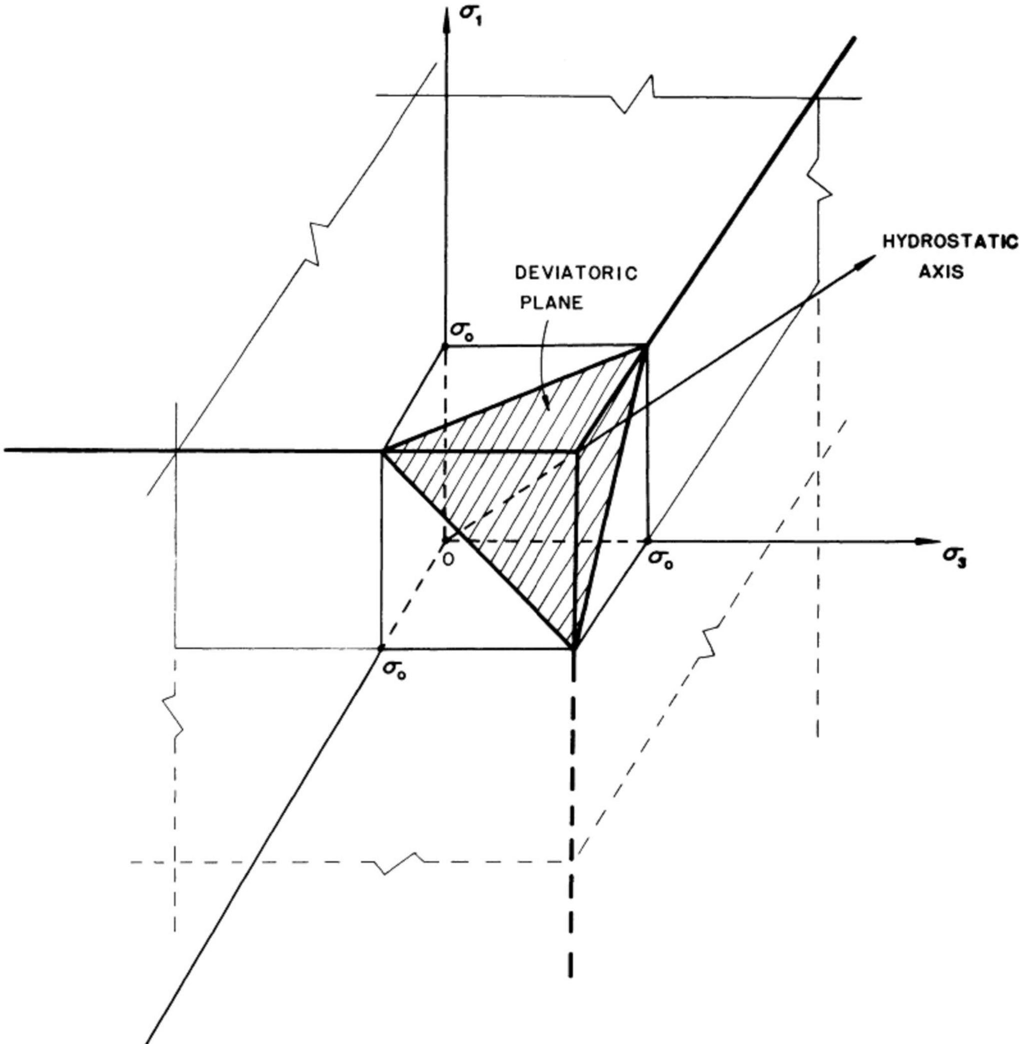

(a)

FIGURE 2.20. (a) Rankine maximum-principal-stress criterion; cross sections of Rankine criterion: (b) meridian plane ($\theta = 0°$); (c) π-plane. Figure continues on next page.

and σ_3, which is a pure shear state $\frac{1}{2}(\sigma_1 - \sigma_3, 0, \sigma_3 - \sigma_1)$ with a hydrostatic stress state $\frac{1}{2}(\sigma_1 + \sigma_3)$ superimposed.

Based on the above considerations, a general shape of the failure surface for an isotropic material may be illustrated in Haigh–Westergaard stress space as shown in Fig. 2.19a. We shall consider this in more detail in the following discussion of some simple failure criteria.

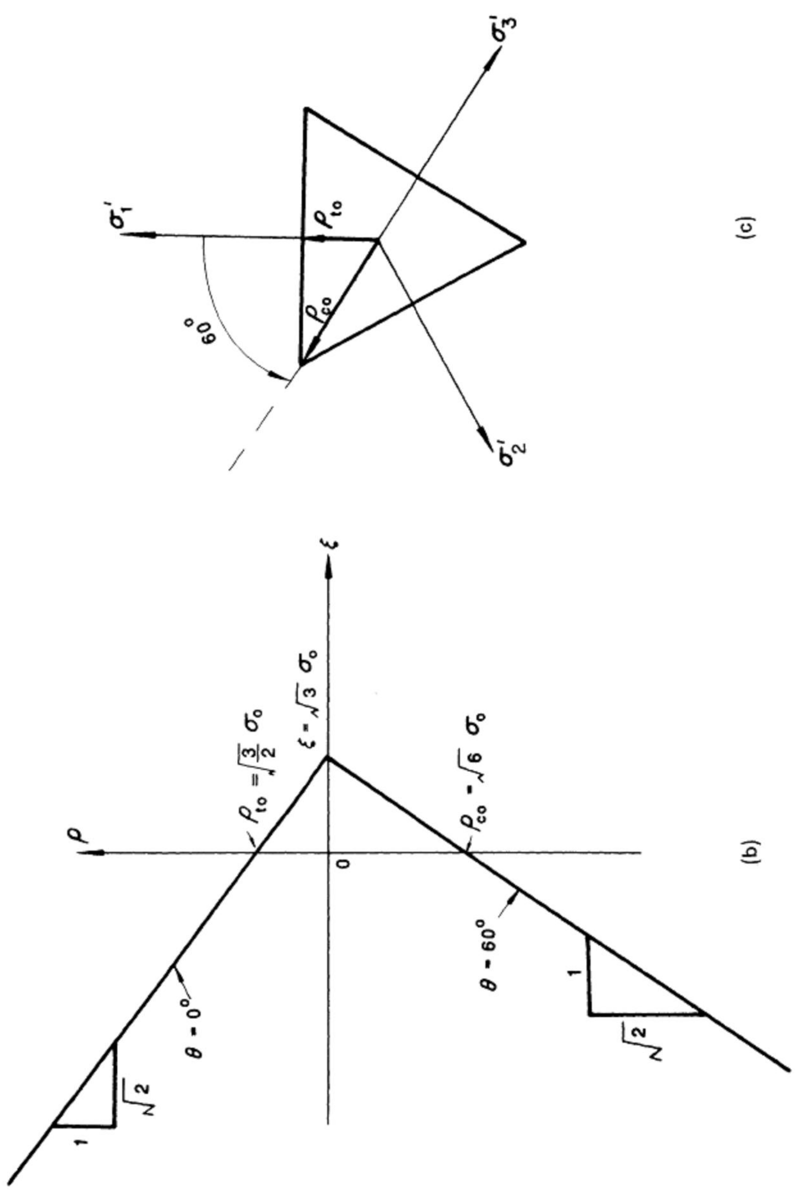

FIGURE 2.20. (b) and (c).

2.3.2. The Maximum-Tensile-Stress Criterion (Rankine)

The maximum-tensile-stress criterion of Rankine, dating from 1876, is generally accepted today to determine whether a tensile failure has occurred for a brittle material. According to this criterion, brittle failure takes place when the maximum principal stress at a point inside the material reaches a value equal to the tensile strength σ_0 as found in a simple tension test, regardless of the normal or shearing stresses that occur on other planes through this point. The equations for the failure surface defined by this criterion are

$$\sigma_1 = \sigma_0, \qquad \sigma_2 = \sigma_0, \qquad \sigma_3 = \sigma_0 \tag{2.168}$$

which result in three planes perpendicular to the σ_1, σ_2, and σ_3 axes, respectively as shown in Fig. 2.20a. This surface will be referred to as the tension-failure surface or the simple *tension cutoff*. When the variables ξ, ρ, θ or I_1, J_2, θ are used, the failure surface can be fully described by the following equations within the range $0 \le \theta \le 60°$ using Eq. (2.123).

$$f(I_1, J_2, \theta) = 2\sqrt{3J_2}\cos\theta + I_1 - 3\sigma_0 = 0 \tag{2.169}$$

or identically

$$f(\xi, \rho, \theta) = \sqrt{2}\rho\cos\theta + \xi - \sqrt{3}\sigma_0 = 0 \tag{2.170}$$

Figures (2.20b and c) show the cross-sectional shape on the π-plane ($\xi = 0$) and the tensile ($\theta = 0°$) and compressive ($\theta = 60°$) meridians of the failure surface.

As we know, some of the nonmetallic materials, such as concrete, rocks, and soils, have a good compressive strength. Under compression loading with confining pressure, this kind of material may even exhibit some ductile and shear failure behavior. Under tension loads, however, a brittle failure behavior with a very low tensile strength is generally observed. Hence, the Rankine criterion is sometimes combined with the Tresca or the von Mises criterion to approximate the failure behavior of such materials. The combined criteria are referred to as the Tresca or the von Mises criterion with a tension cutoff, and their graphical representations consist of two surfaces, corresponding to a combined behavior of shear failure in compression and tensile failure in tension. An example of such failure surfaces is shown in Fig. 2.21, in which the compressive strength is assumed three times as large as the tensile strength.

2.3.3. The Mohr–Coulomb Criterion

Mohr's criterion, dating from 1900, may be considered as a generalized version of the Tresca criterion. Both criteria are based on the assumption that the maximum shear stress is the only decisive measure of impending failure. However, while the Tresca criterion assumes that the critical value

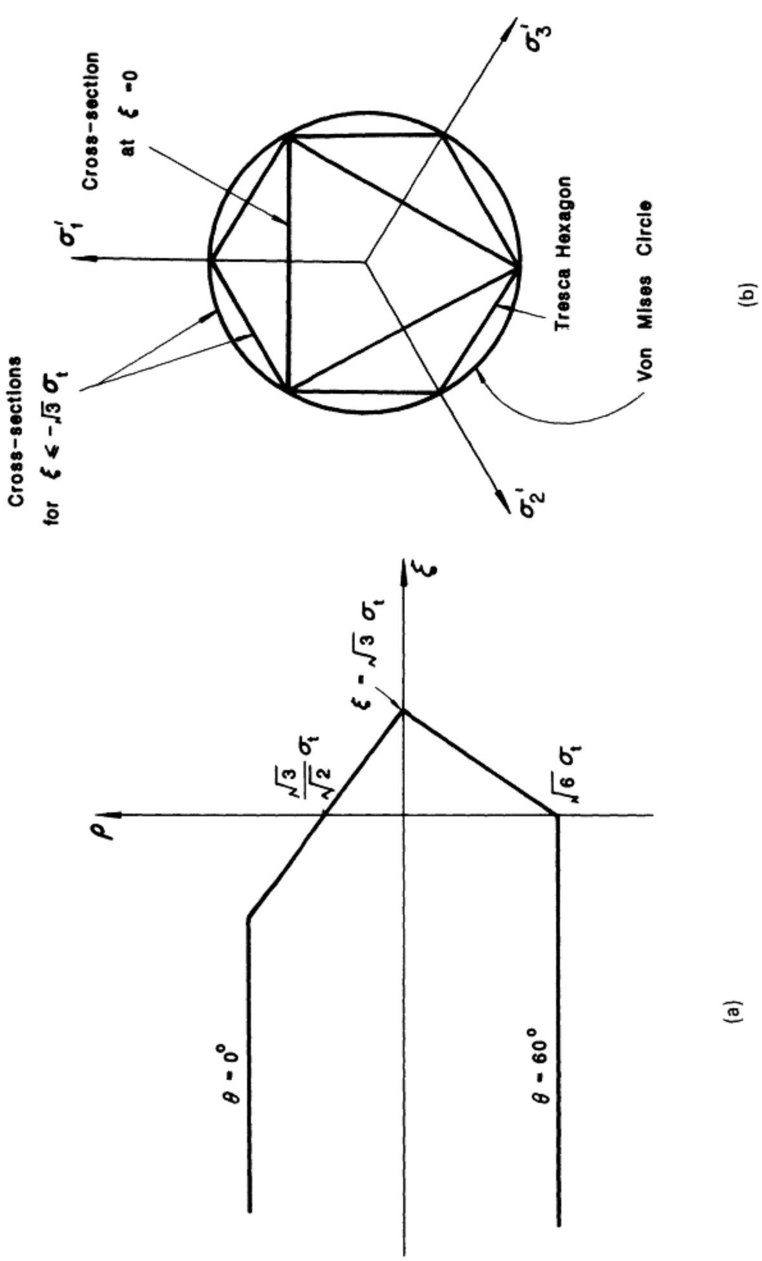

FIGURE 2.21. Tresca and von Mises criteria with tension cutoff: (a) meridian section ($\theta = 0°$); (b) cross sections.

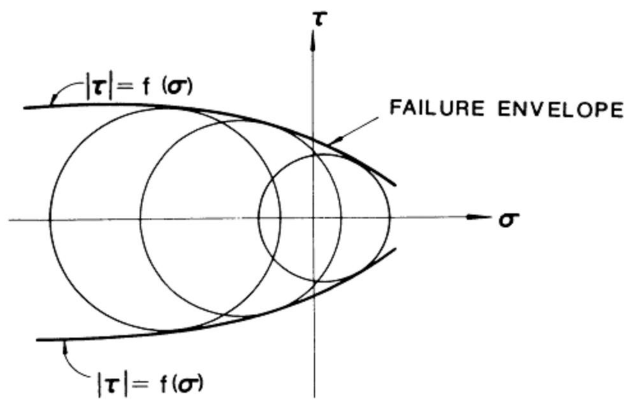

FIGURE 2.22. Graphical representation of Mohr's criterion.

of the shear stress is a constant, Mohr's failure criterion considers the limiting shear stress τ in a plane to be a function of the normal stress σ in the same plane at a point, i.e.,

$$|\tau| = f(\sigma) \tag{2.171}$$

where $f(\sigma)$ is an experimentally determined function.

In terms of Mohr's graphical representation of the state of stress, Eq. (2.171) means that failure of material will occur if the radius of the largest principal circle is tangent to the envelope curve $f(\sigma)$ as shown in Fig. 2.22. In constrast to the Tresca criterion, it is seen that Mohr's criterion allows for the effect of the mean stress or the hydrostatic stress.

The simplest form of the Mohr envelope $f(\sigma)$ is a straight line, illustrated in Fig. 2.23. The equation for the straight-line envelope is known as Coulomb's equation, dating from 1773,

$$|\tau| = c - \sigma \tan \phi \tag{2.172}$$

in which c is the cohesion and ϕ is the angle of internal friction; both are material constants determined by experiment. The failure criterion associated with Eq. (2.172) will be referred to as the Mohr–Coulomb criterion. In the special case of frictionless materials, for which $\phi = 0$, Eq. (2.172) reduces to the maximum-shear-stress criterion of Tresca, $\tau = c$, and the cohesion becomes equal to the yield stress in pure shear $c = k$.

From Eq. (2.172) and for $\sigma_1 \geq \sigma_2 \geq \sigma_3$, the Mohr–Coulomb criterion can be written as

$$\frac{1}{2}(\sigma_1 - \sigma_3) \cos \phi = c - \left[\frac{1}{2}(\sigma_1 + \sigma_3) + \frac{\sigma_1 - \sigma_3}{2} \sin \phi\right] \tan \phi \tag{2.173}$$

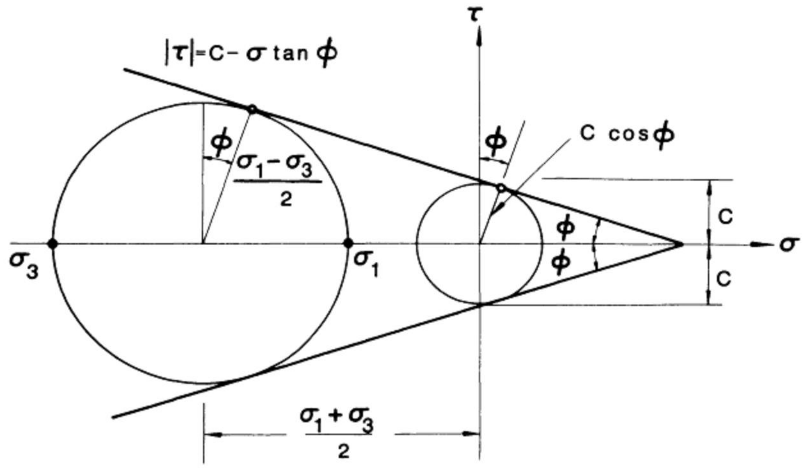

FIGURE 2.23. Mohr-Coulomb criterion: with straight line as failure envelope.

or rearranging

$$\sigma_1 \frac{1+\sin\phi}{2c\cos\phi} - \sigma_3 \frac{1-\sin\phi}{2c\cos\phi} = 1 \tag{2.174}$$

If we define

$$f'_c = \frac{2c\cos\phi}{1-\sin\phi} \tag{2.175}$$

and

$$f'_t = \frac{2c\cos\phi}{1+\sin\phi} \tag{2.176}$$

Eq. (2.174) is further reduced to

$$\frac{\sigma_1}{f'_t} - \frac{\sigma_3}{f'_c} = 1 \qquad \text{for } \sigma_1 \geq \sigma_2 \geq \sigma_3 \tag{2.177}$$

It is clear from Eq. (2.177) that f'_t is the strength in simple tension while f'_c is the strength in simple compression.

It is sometimes convenient to introduce a parameter m, where

$$m = \frac{f'_c}{f'_t} = \frac{1+\sin\phi}{1-\sin\phi} \tag{2.178}$$

Then Eq. (2.177) can be written in the slope-intercept form

$$m\sigma_1 - \sigma_3 = f'_c \qquad \text{for } \sigma_1 \geq \sigma_2 \geq \sigma_3 \tag{2.179}$$

Similarly to what we have done for the Tresca criterion, $\sigma_1 - \sigma_3 = \sigma_0$, the failure locus for the Mohr-Coulomb criterion in the $\sigma_1 - \sigma_2$ plane can be sketched based on Eq. (2.179) for several values of m. The failure loci are irregular hexagons as shown in Fig. 2.24.

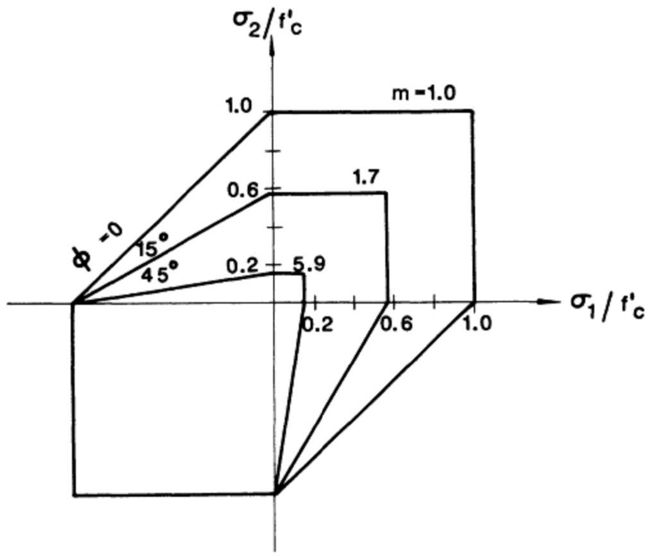

FIGURE 2.24. Mohr–Coulomb criterion in the coordinate plane $\sigma_3 = 0$.

To demonstrate the shape of the three-dimensional failure surface of the Mohr–Coulomb criterion, we again use Eq. (2.123) and rewrite Eq. (2.174) in the following form:

$$f(I_1, J_2, \theta) = \frac{1}{3} I_1 \sin\phi + \sqrt{J_2} \sin\left(\theta + \frac{\pi}{3}\right) + \frac{\sqrt{J_2}}{\sqrt{3}} \cos\left(\theta + \frac{\pi}{3}\right) \sin\phi - c\cos\phi = 0 \tag{2.180}$$

or identically in terms of variables ξ, ρ, θ:

$$f(\xi, \rho, \theta) = \sqrt{2}\xi \sin\phi + \sqrt{3}\rho \sin\left(\theta + \frac{\pi}{3}\right) + \rho\cos\left(\theta + \frac{\pi}{3}\right) \sin\phi - \sqrt{6}c\cos\phi = 0 \tag{2.181}$$

with $0 \leq \theta \leq \pi/3$.

In principal stress space, this gives an irregular hexagonal pyramid. Its meridians are straight lines (Fig. 2.25a), and its cross section in the π-plane is an irregular hexagon (Fig. 2.25b). Only two characteristic lengths are required to draw this hexagon: the lengths ρ_{t0} and ρ_{c0}, which can be obtained directly from Eq. (2.181) with $\xi = 0$, $\theta = 0°$, $\rho = \rho_{t0}$ and $\xi = 0$, $\theta = 60°$, $\rho = \rho_{c0}$. Using Eqs. (2.175) and (2.176), we have the following alternative forms for

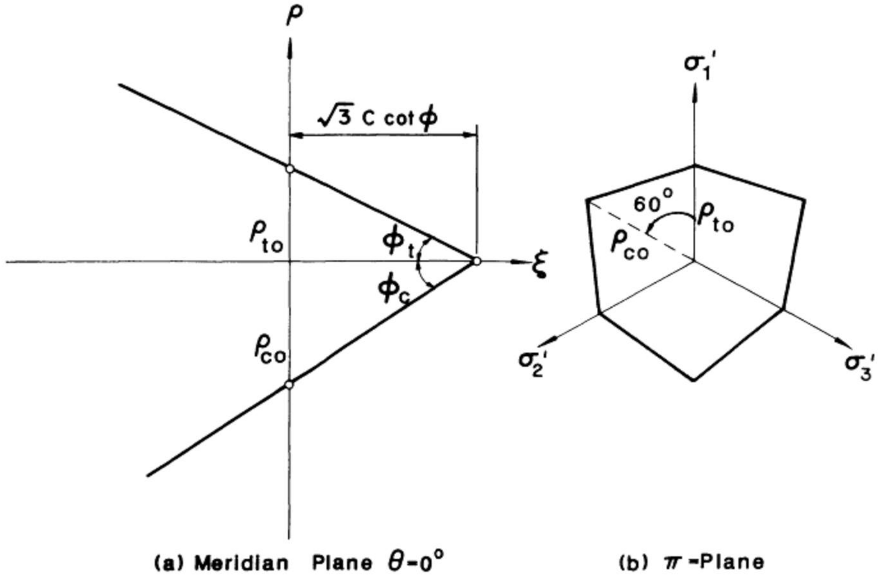

FIGURE 2.25. Graphical representation of Mohr–Coulomb criterion in principal stress space.

ρ_{t0} and ρ_{c0} on the π-plane:

$$\rho_{t0}=\frac{2\sqrt{6}c\cos\phi}{3+\sin\phi}=\frac{\sqrt{6}f_c'(1-\sin\phi)}{3+\sin\phi} \tag{2.182}$$

$$\rho_{c0}=\frac{2\sqrt{6}c\cos\phi}{3-\sin\phi}=\frac{\sqrt{6}f_c'(1-\sin\phi)}{3-\sin\phi} \tag{2.183}$$

and the ratio of these lengths is given by

$$\frac{\rho_{t0}}{\rho_{c0}}=\frac{3-\sin\phi}{3+\sin\phi} \tag{2.184}$$

A family of Mohr–Coulomb cross sections in the π-plane for several values of ϕ is shown in Fig. 2.26, where the stresses have been normalized with respect to the compressive strength f_c'. Obviously, the hexagons shown in Fig. 2.24 are the intersections of the pyramid with the coordinate plane $\sigma_3=0$. When $f_c'=f_t'$ (or equivalently, when $\phi=0$ or $m=1$), the hexagon becomes identical with Tresca's hexagon, as it should.

To obtain a better approximation when tensile stresses occur, it is sometimes necessary to combine the Mohr–Coulomb criterion with a maximum-tensile-strength cutoff. It should be noted that this combined criterion is a three-parameter criterion. We need two stress states to determine the values of c and ϕ and one stress state to determine the maximum tensile stress.

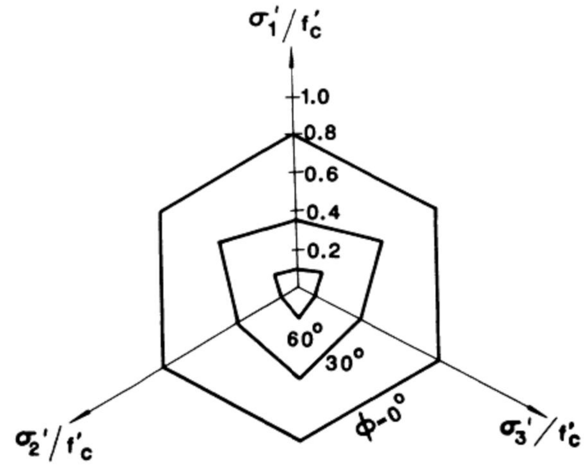

FIGURE 2.26. Failure curves for Mohr-Coulomb criterion in the deviatoric planes.

2.3.4. The Drucker-Prager Criterion

As we have seen, the Mohr-Coulomb failure criterion can be considered a generalized Tresca criterion accounting for the hydrostatic pressure effect. The Drucker-Prager criterion, formulated in 1952, is a simple modification of the von Mises criterion, where the influence of a hydrostatic stress component on failure is introduced by inclusion of an additional term in the von Mises expression to give

$$f(I_1, J_2) = \alpha I_1 + \sqrt{J_2} - k = 0 \tag{2.185}$$

Using variables ξ and ρ leads to

$$f(\xi, \rho) = \sqrt{6}\alpha\xi + \rho - \sqrt{2}k = 0 \tag{2.186}$$

where α and k are material constants. When α is zero, Eq. (2.186) reduces to the von Mises criterion.

The failure surface of Eq. (2.186) in principal stress space is clearly a right-circular cone. Its meridian and cross section on the π-plane are shown in Fig. 2.27.

The Mohr-Coulomb hexagonal failure surface is mathematically convenient only in problems where it is obvious which one of the six sides is to be used. If this information is not known in advance, the corners of the hexagon can cause considerable difficulty and give rise to complications in obtaining a numerical solution. The Drucker-Prager criterion, as a smooth approximation to the Mohr-Coulomb criterion, can be made to match the latter by adjusting the size of the cone. For example, if the Drucker-Prager circle is made to agree with the outer apices of the Mohr-Coulomb hexagon, i.e., the two surfaces are made to coincide along the compression meridian

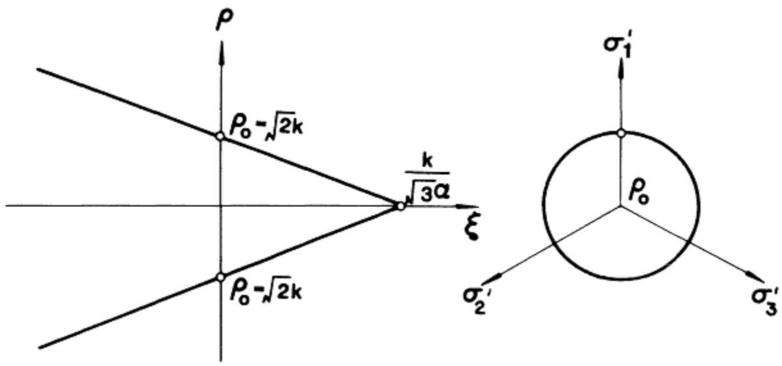

FIGURE 2.27. Drucker–Prager criterion: (a) meridian plane, $\theta=0°$; (b) π-plane.

ρ_c, where $\theta=60°$, then the constants α and k in Eq. (2.185) are related to the constants c and ϕ in Eq. (2.174) by

$$\alpha=\frac{2\sin\phi}{\sqrt{3}(3-\sin\phi)},\qquad k=\frac{6c\cos\phi}{\sqrt{3}(3-\sin\phi)} \tag{2.187}$$

The cone corresponding to the constants in Eq. (2.187) circumscribes the hexagonal pyramid and represents an outer bound on the Mohr–Coulomb failure surface (Fig. 2.28). On the other hand, the inner cone passes through the tension meridian ρ_t, where $\theta=0$, and will have the constants

$$\alpha=\frac{2\sin\phi}{\sqrt{3}(3+\sin\phi)},\qquad k=\frac{6c\cos\phi}{\sqrt{3}(3+\sin\phi)} \tag{2.188}$$

However, the approximation given by either the inner or the outer cone to the Mohr–Coulomb failure surface can be poor for certain stress states. Other approximations made to match another meridian, say, the shear meridian, may be better.

The Drucker–Prager criterion for a biaxial stress state is represented by the intersection of the circular cone with the coordinate plane of $\sigma_3=0$. Substituting $\sigma_3=0$ into Eq. (2.185) leads to

$$\alpha(\sigma_1+\sigma_2)+\sqrt{\tfrac{1}{3}(\sigma_1^2-\sigma_1\sigma_2+\sigma_2^2)}=k \tag{2.189}$$

or rearranging

$$(1-3\alpha^2)(\sigma_1^2+\sigma_2^2)-(1+6\alpha^2)\sigma_1\sigma_2+6k\alpha(\sigma_1+\sigma_2)-3k^2=0 \tag{2.190}$$

which is an off-center ellipse as shown in Fig. 2.29.

EXAMPLE 2.6. A material has a tensile strength f_t' equal to one-tenth of its compressive strength f_c'. Consider a material element subjected to a combination of normal stress σ and shear stress τ. On the basis of (a) the

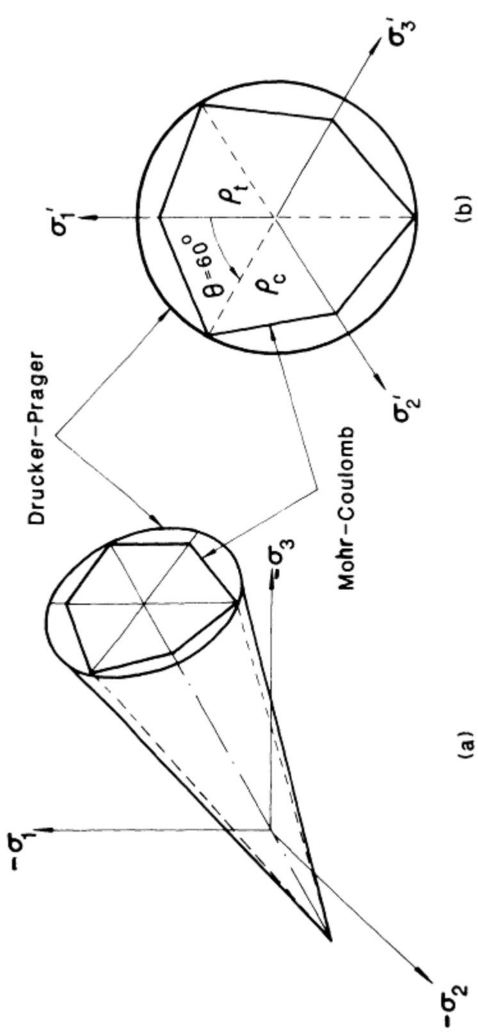

FIGURE 2.28. Drucker–Prager and Mohr–Coulomb criteria matched along the compressive meridian: (a) in principal stress space; (b) in the deviatoric plane.

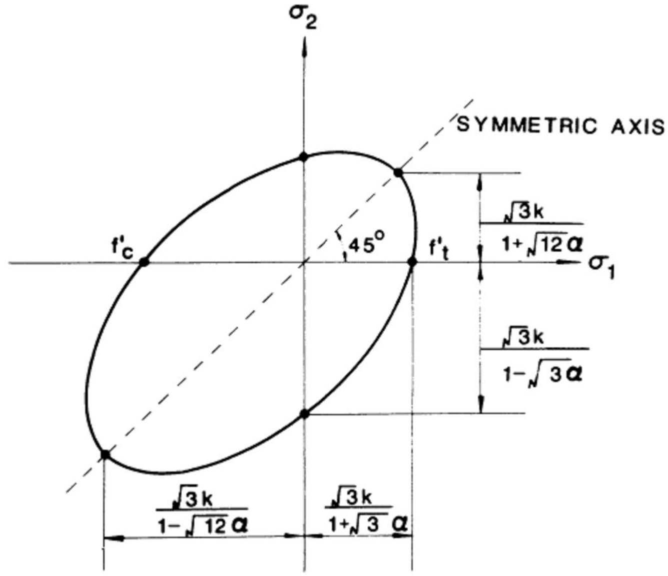

FIGURE 2.29. Drucker-Prager criterion in the coordinate plane $\sigma_3 = 0$.

Mohr-Coulomb criterion and (b) the Drucker-Prager criterion, sketch the interaction curves which govern the failure of the element.

SOLUTION. (a) Mohr-Coulomb criterion: To use the failure condition of Eq. (2.177), we must find the principal stresses from Mohr's circle as

$$\begin{aligned} \frac{\sigma}{2} + \sqrt{\left(\frac{\sigma}{2}\right)^2 + \tau^2} &= \sigma_1 > 0 \\ \frac{\sigma}{2} - \sqrt{\left(\frac{\sigma}{2}\right)^2 + \tau^2} &= \sigma_3 < 0 \end{aligned} \tag{2.191}$$

and the stress in the direction perpendicular to the σ_1-σ_3 plane is zero,

$$\sigma_2 = 0$$

Substituting Eq. (2.191) into Eq. (2.177) yields

$$\frac{\sigma + \sqrt{\sigma^2 + 4\tau^2}}{2f'_t} - \frac{\sigma - \sqrt{\sigma^2 + 4\tau^2}}{2f'_c} = 1 \tag{2.192}$$

Noting that $f'_t = \frac{1}{10} f'_c$ and rearranging, one gets

$$\left[\frac{\sigma + \frac{9}{20} f'_c}{\frac{11}{20} f'_c}\right]^2 + \left(\frac{\tau}{f'_c/\sqrt{40}}\right)^2 = 1 \tag{2.193}$$

which is an ellipse as shown in Fig. 2.30.

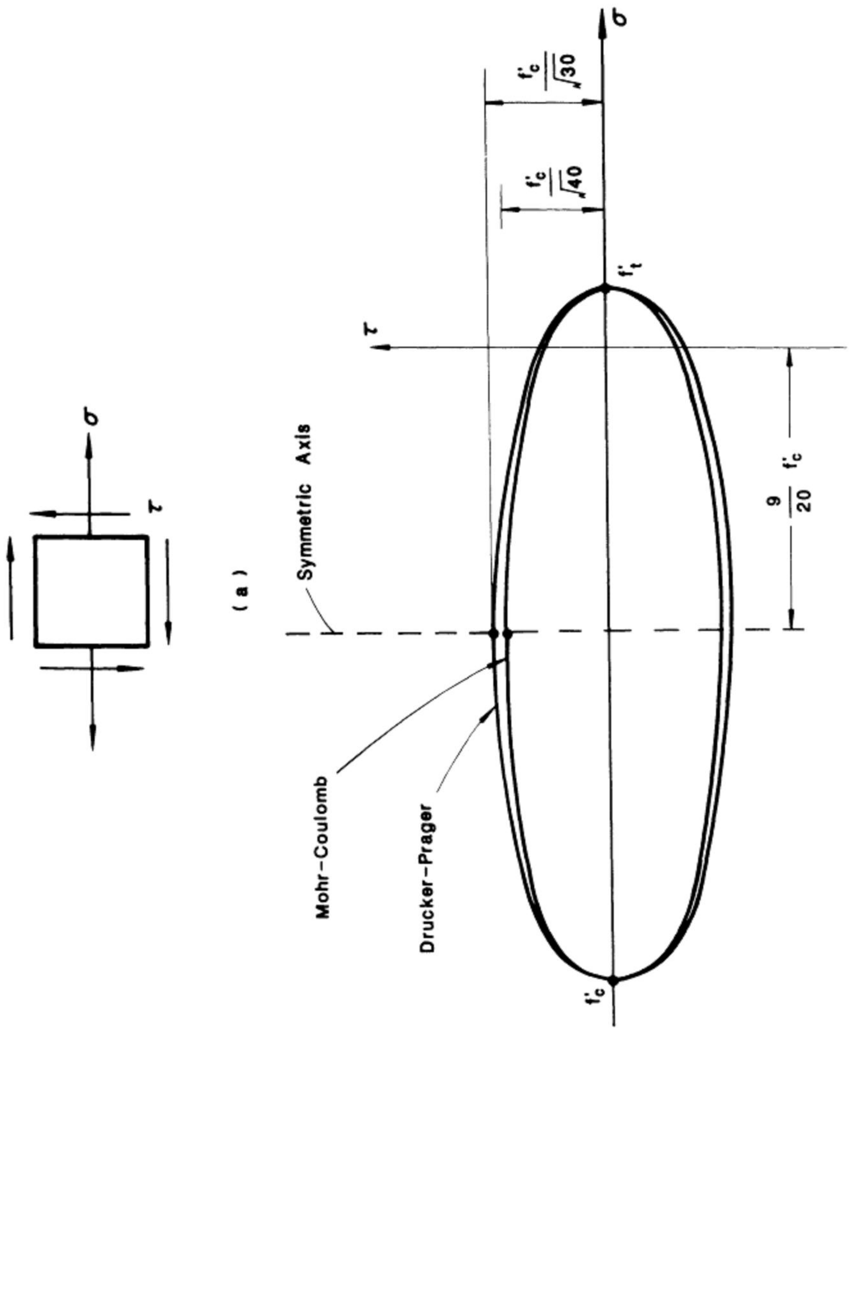

FIGURE 2.30. (a) An element subjected to normal stress σ and shear stress τ. (b) Failure curves based on Mohr–Coulomb and Drucker–Prager criteria.

(b) Drucker–Prager criterion: The material constants α and k can be determined from the given tensile failure stress f'_t and compression failure strength f'_c. Substituting stress states ($\sigma_1 = f'_t$, $\sigma_2 = \sigma_3 = 0$) and ($\sigma_1 = \sigma_2 = 0$, $\sigma_3 = -f'_c$) into the failure condition of Eq. (2.185), one gets

$$\begin{aligned} \alpha f'_t + \frac{1}{\sqrt{3}} f'_t - k = 0 \\ -\alpha f'_c + \frac{1}{\sqrt{3}} f'_c - k = 0 \end{aligned} \tag{2.194}$$

Noting that $f'_c = 10 f'_t$ and solving Eq. (2.194) for k and α leads to

$$k = \frac{2}{11\sqrt{3}} f'_c, \qquad \alpha = \frac{9}{11\sqrt{3}} \tag{2.195}$$

For the stress state (σ, τ), $I_1 = \sigma$, $J_2 = \frac{1}{3}\sigma^2 + \tau^2$, Eq. (2.185) becomes

$$\alpha\sigma + \sqrt{\tfrac{1}{3}\sigma^2 + \tau^2} - k = 0 \tag{2.196}$$

Substituting Eq. (2.195) into Eq. (2.196) and rearranging, we obtain the failure condition for the given stress state as

$$\left[\frac{\sigma + \frac{9}{20} f'_c}{\frac{11}{20} f'_c}\right]^2 + \left[\frac{\tau}{f'_c/\sqrt{30}}\right]^2 = 1 \tag{2.197}$$

which is also an ellipse as shown in Fig. 2.30.

2.4. Anisotropic Failure/Yield Criteria

Although most materials can be treated as isotropic approximately, strictly speaking, all materials are anisotropic to some extent; that is, the material properties are not the same in every direction. The general form of the failure/yield criteria for anisotropic materials has been expressed by Eq. (2.130). However, the definite form of the function $f(\sigma_{ij}, k_1, k_2, \ldots)$ depends very much on the characteristics of the material.

2.4.1. A Yield Criterion for Orthotropic Materials

An orthotropic material has three mutually orthogonal planes of symmetry at every point. The intersection of these planes are known as the principal axes of anisotropy. The yield criterion proposed by Hill (1950), when referred to these axes, has the form

$$\begin{aligned} f(\sigma_{ij}) = a_1(\sigma_y - \sigma_z)^2 + a_2(\sigma_z - \sigma_x)^2 + a_3(\sigma_x - \sigma_y)^2 \\ + a_4\tau_{yz}^2 + a_5\tau_{zx}^2 + a_6\tau_{xy}^2 - 1 = 0 \end{aligned} \tag{2.198}$$

where $a_1, a_2, \ldots, a_6$ are material parameters. Equation (2.198) is a quadratic expression of the stresses, representing some kind of energy that governs yielding of the orthotropic materials. The Hill criterion is therefore considered an extended form of the distortion-energy criterion of von Mises. The omission of the linear terms and the appearance of only differences between normal stress components in the yield criterion implies the assumptions that the material responses are equal in tension and compression and that a hydrostatic stress does not influence yielding.

The material parameters may be determined from three simple tension tests in the directions of the principal axes of anisotropy and three simple shear tests along the planes of symmetry. Denote the tensile strengths as X, Y, and Z, corresponding to the x-, y-, and z-axes, and the shear strengths as S_{23}, S_{31}, and S_{12}, corresponding to the three coordinate planes. Substituting these six states of stress into Eq. (2.198) and solving for the parameters, we obtain

$$\begin{aligned}
2a_1 &= \frac{1}{Y^2}+\frac{1}{Z^2}-\frac{1}{X^2} \\
2a_2 &= \frac{1}{Z^2}+\frac{1}{X^2}-\frac{1}{Y^2} \\
2a_3 &= \frac{1}{X^2}+\frac{1}{Y^2}-\frac{1}{Z^2} \\
a_4 &= \frac{1}{S_{23}^2} \\
a_5 &= \frac{1}{S_{31}^2} \\
a_6 &= \frac{1}{S_{12}^2}
\end{aligned} \tag{2.199}$$

If the material is transversely isotropic (rotational symmetry about the z-axis), Eq. (2.198) must remain invariant for arbitrary x-, y-axes of reference. It follows that the parameters must satisfy the relations:

$$a_1 = a_2, \qquad a_4 = a_5, \qquad a_6 = 2(a_1 + 2a_3) \tag{2.200}$$

For a complete isotropy,

$$6a_1 = 6a_2 = 6a_3 = a_4 = a_5 = a_6 \tag{2.201}$$

and Eq. (2.198) reduces to the von Mises criterion.

2.4.2. A Criterion for Ice Crushing Failure

Ice is columnar-grained in structure. It may be treated as an orthotropic material. However, the strength of ice is sensitive to hydrostatic pressure. Its tensile strength is much lower than its compressive strength. The Hill criterion of Eq. (2.198) cannot model such behavior, and therefore, is not